Transition Met Chem (2012) 37:345–359
DOI 10.1007/s11243-012-9595-2

3D sandwich-like frameworks constructed from silver chains: synthesis and crystal structures of six silver(I) coordination complexes

Chong-chen Wang · Peng Wang · Guang-Liang Guo

Received: 14 January 2012 / Accepted: 1 March 2012 / Published online: 22 March 2012

Abstract The reaction of $AgNO_3$ with combinations of 4,4′-bipyridine (bpy), 1,2-di(4-pyridyl)ethane (dpe), 1,3-bis(4-pyridyl)propane (bpp), succinic acid (H_2su), terephthalic acid (H_2tp), 2,2′-diphenylaminedicarboxylic acid (H_2dpadc), and naphthaleneacetic acid (Hnaa) in aqueous alcohol at room temperature produces block-like crystals of $[Ag_3(bpy)_3](su)\cdot 10H_2O$, $[Ag_2(bpy)_2](tp)\cdot 6H_2O$, $[Ag_2(dpe)_2(H_2O)_2](dpadc)\cdot H_2O$, $[Ag_6(dpe)_6(H_2O)_4](tp)_3\cdot 12H_2O$, [Ag(bpp)](naa), and $[Ag_2(bpp)_2](dpadc)\cdot 6H_2O$. All six compounds consist of 1D infinite silver-bpy/dpe/bpp cationic chains, interspersed with organic carboxylate anions that provide charge compensation in the crystal structures. The lattice water molecules are situated among the framework of the crystal structure and show rich hydrogen-bonding interactions {except for [Ag(bpp)](naa)}, which help to orientate of the organic carboxylate anions in the crystal packing.

Introduction

The growing interest in the design and assembly of silver-based coordination complexes is not only because of their fascinating molecular structures [1–4], but also because of their distinctive chemical and physical properties [5–16]. The geometrical flexibility of silver(I) results in intricate coordination architectures and also affords an opportunity to explore how the self-assembly of silver-based coordination compounds can be influenced by factors such as the structural characteristics of polydentate organic ligands, the metal–ligand ratio, solvents, and the counterions [1–4, 9–11]. It is noteworthy that counterions, especially anions, often play important roles in determining the structures of silver-based coordination compounds. The commonly used anions include BF_4^-, ClO_4^-, PF_6^-, NO_3^-, $CF_3SO_3^-$, and $CF_3CO_2^-$, which can participate in coordinated, uncoordinated, or mixed modes [17, 18]. The size, coordination ability, and supramolecular interactions of these anions exert different influences on the final Ag(I) coordination compounds. Compared to inorganic anions, the organic carboxylate anions are more numerous and versatile; we have, therefore, chosen to focus our efforts on the synthesis of silver complexes containing different organic carboxylate anions in order to explore how the self-assembly process can be influenced by these organic anions [2–4, 19].

Herein, we present six silver coordination compounds, namely $[Ag_3(bpy)_3](su)\cdot 10H_2O$ (1), $[Ag_2(bpy)_2](tp)]\cdot 6H_2O$ (2), $[Ag_2(dpe)_2(H_2O)_2](dpadc)\cdot H_2O$ (3), $[Ag_6(dpe)_6(H_2O)_4](tp)_3\cdot 12H_2O$ (4), [Ag(bpp)](naa) (5), and $[Ag_2(bpp)_2](dpadc)\cdot 6H_2O$ (6) constructed via self-assembly of silver(I) metal salts with N-donor ligands, namely 4,4′-bipyridine (bpy), 1,2-di(4-pyridyl)ethane (dpe) and 1,3-bis(4-pyridyl)-propane (bpp), and organic carboxylate anions, like succinic acid (H_2su), terephthalic acid (H_2tp), 2,2′-diphenylaminedicarboxylic acid (H_2dpadc), and naphthaleneacetic acid (Hnaa) (Scheme 1), in order to investigate the influence of rigid and flexible N-donor ligands and organic carboxylate anions on the crystal structures of the resulting silver-based coordination compounds.

Experimental

All chemicals were commercially available reagent grade and used without further purification. Elemental analysis for

C. Wang (✉) · P. Wang · G.-L. Guo
Key Laboratory of Urban Stormwater System and Water Environment (Ministry of Education), Beijing University of Civil Engineering and Architecture, Beijing 100044, China
e-mail: chongchenwang@126.com

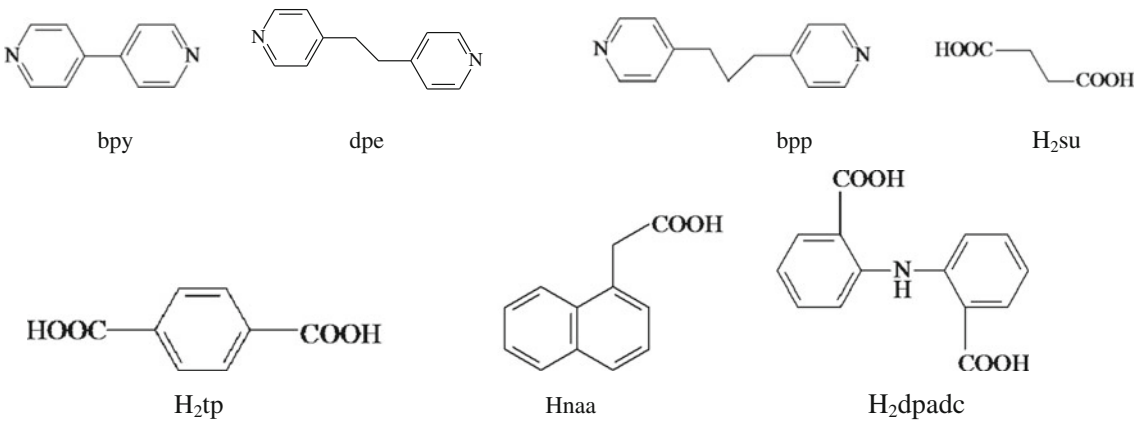

Scheme 1 The structural formulae of bpy, dpe, bpp, H_2su, H_2tp, Hnaa, and H_2bpadc

the title complexes was performed using an Elementar Vario EL-III instrument. FTIR spectra, in the region (400–4,000 cm^{-1}), were recorded on a Perkin Elmer Spectrum 100 Fourier Transform infrared spectrophotometer.

Synthesis of $[Ag_3(bpy)_3](su)\cdot 10H_2O$ (1)

An ammonia solution (25 mL, 0.5 mol/L) containing $AgNO_3$ (0.0085 g, 0.05 mmol) and H_2su (0.006 g, 0.05 mmol) was added dropwise to an EtOH solution (25 mL) of bpy (0.0078 g, 0.05 mmol). The clear mixture was stirred for a few minutes and then allowed to evaporate slowly at room temperature. Block-like colorless crystals of $[Ag_3(bpy)_3](su)\cdot 10H_2O$ (1) were obtained after several weeks. Anal. Calcd. for $C_{36}H_{50}Ag_3N_6O_{16}$ (%): C, 37.7; H, 4.4; N, 7.3. Found: C, 37.8; H, 4.5; N, 7.3. IR (KBr)/cm^{-1}: 3405 m, 3030w, 2947w, 2925w, 2859w, 1933w, 1605s, 1558s, 1494s, 1414m, 1295m, 1218m, 1177w, 1076w, 1012w, 991w, 918m, 881m, 827m, 808m, 655m, 610w, 546m, 423m, 408m.

Synthesis of $[Ag_2(bpy)_2](tp)]\cdot 6H_2O$ (2)

Synthesis of block-like colorless crystals of $[Ag_2(bpy)_2](tp)]\cdot 6H_2O$ (2) followed the same procedure as for 1, except that H_2su was replaced with H_2tp. Anal. Calcd. for $C_{28}H_{30}Ag_2N_4O_{10}$ (%): C, 42.1; H, 3.8; N, 7.0. Found: C, 42.2; H, 3.8; N, 7.1. IR (KBr)/cm^{-1}: 3402m, 3051m, 3028m, 1953w, 1598s, 1573s, 1526m, 1496m, 1487w, 1399s, 1376s, 1313w, 1222m, 1089m, 1040w, 1071w, 1013w, 1001w, 993w, 962w, 883w, 846m, 824s, 805s, 743s, 621s, 564m, 508s, 451w.

Synthesis of $[Ag_2(dpe)_2(H_2O)_2](dpadc)\cdot H_2O$ (3)

Synthesis of block-like colorless crystals of $[Ag_2(dpe)_2(H_2O)_2](dpadc)\cdot H_2O$ (3) followed the same procedure as for 1, except that H_2su and bpy were replaced with H_2dpadc and dpe, respectively. Anal. Calcd. for $C_{38}H_{35}Ag_2N_5O_7$ (%): C, 45.7; H, 4.2; N, 6.7. Found: C, 45.8; H, 4.2; N, 6.7. IR (KBr)/cm^{-1}: 3433s, 1601s, 1571m, 1557s, 1498m, 1450w, 1384s, 1272m, 1204w, 1146w, 1073w, 1042w, 1009w, 997m, 972m, 848w, 826m, 735m, 697w, 548m, 405m.

Synthesis of $[Ag_6(dpe)_6(H_2O)_4](tp)_3\cdot 12H_2O$ (4)

Synthesis of block-like colorless crystals of $[Ag_6(dpe)_6(H_2O)_4](tp)_3\cdot 12H_2O$ (4) followed the same procedure as for 1, except that H_2su and bpy were replaced with H_2tp and dpe, respectively. Anal. Calcd. for $C_{96}H_{104}Ag_6N_{12}O_{28}$ (%): C, 44.9; H, 2.8; N, 8.7. Found: C, 44.9; H, 2.9; N, 8.8. IR (KBr)/cm^{-1}: 3272m, 2926w, 2861w, 1936w, 1604s, 1561s, 1519m, 1498m, 1455w, 1434m, 1407s, 1377s, 1296m, 1218m, 1100m, 1075w, 1012w, 1006w, 991m, 926m, 860m, 831m, 809m, 802m, 778m, 754w, 726s, 613m, 603w, 577m, 507m, 404m.

Synthesis of [Ag(bpp)](naa) (5)

Synthesis of block-like colorless crystals of [Ag(bpp)](naa) (5) followed the same procedure as for 1, except that H_2su and bpy were replaced with H_2naa and bpp, respectively. Anal. Calcd. for $C_{25}H_{23}AgN_2O_2$ (%): C, 61.1; H, 4.7; N, 5.7. Found: C, 61.2; H, 4.8; N, 5.7. IR (KBr)/cm^{-1}: 3416m, 2926w, 2860w, 1604s, 1565s, 1497w, 1455w, 1421m, 1384s, 1257w, 1219w, 1075w, 1006w, 802m, 793m, 785m, 613w, 538w, 512m, 417w.

Synthesis of $[Ag_2(bpp)_2](dpadc)\cdot 6H_2O$ (6)

Synthesis of block-like colorless crystals of $[Ag_2(bpp)_2](dpadc)\cdot 6H_2O$ (6) followed the same procedure as for 1, except that H_2su and bpy were replaced with H_2naa and

bpp, respectively. Anal. Calcd. for $C_{40}H_{49}Ag_2N_5O_{10}$ (%): C, 49.3; H, 5.1; N, 7.2. Found: C, 49.3; H, 5.1; N, 7.2. IR (KBr)/cm^{-1}: 3436m, 1604s, 1571s, 1558s, 1499s, 1455w, 1420m, 1393s, 1273m, 1219w, 1210w, 1148w, 1070w, 1041w, 1024w, 1006w, 849m, 809m, 802m, 753m, 734m, 698s, 681w, 613w, 512m, 405m.

X-ray crystallography

Diffraction intensities for all six complexes were recorded with a Bruker CCD area detector diffractometer with graphite-monochromatized Mo$K\alpha$ radiation ($\lambda = 0.71073$ Å) using φ-ω mode at 298(2) K. Semi-empirical absorption corrections were applied using the SADABS program [20]. The structures were solved by direct methods [21] and refined by full-matrix least-squares on F^2 using SHELXS 97 and SHELXL 97 programs, respectively [21, 22]. All non-hydrogen atoms were refined anisotropically, and hydrogen atoms were placed in geometrically calculated positions. Crystallographic data and structural refinements for the complexes are summarized in Table 1. Selected bond lengths and angles are listed in Table 2.

Results and discussion

Crystallographic analysis of complex (1)

The crystal structure reveals that $[Ag_3(bpy)_3](su)\cdot 10H_2O$ (1) is made up of infinite chains of $[Ag_3(bpy)_3]_n^{3n+}$ cations, su^{2-} anions, and H_2O molecules, as illustrated in Fig. 1a. In the cationic chains of $[Ag_3(bpy)_3]_n^{3n+}$, both the Ag(1) and Ag(2) atoms have linear coordination geometry involving the nitrogen atoms from two different bpy ligands [Ag–N ranging from 2.153(3) to 2.157(3) Å; N–Ag–N from 159.34(12)° to 166.40(12)°], forming a simple topology of single-strand chain. The Ag(3) atoms, in slightly distorted T-shaped geometry, are coordinated by nitrogens from two different bpy ligands [Ag–N 2.184(3) and 2.193(3) Å; N–Ag–N 170.35(12)°] and by an oxygen atom from a COO^- group [Ag–O 2.483(3) Å; N–Ag–O 99.09(11)° and 96.05(11)°], as illustrated in Fig. 1a and Table 2. The typical ranges of Ag–N and Ag–O bond distances are 2.11–2.63 Å and 2.3–2.6 Å [23–25], respectively. The oxygen atoms of the COO^- groups of the su^{2-} anions interact with the Ag centers through weak Ag…O interactions [Ag(1)…O(1) and Ag(1)…O(2) = 2.708(3)

Table 1 Details of X-ray data collection and refinement for the complexes

	1	2	3	4	5	6
Formula	$C_{36}H_{50}Ag_3N_6O_{16}$	$C_{28}H_{30}Ag_2N_4O_{10}$	$C_{38}H_{35}Ag_2N_5O_7$	$C_{96}H_{104}Ag_6N_{12}O_{28}$	$C_{25}H_{23}AgN_2O_2$	$C_{40}H_{49}Ag_2N_5O_{10}$
M	1,146.43	798.30	889.45	2,521.13	491.32	975.58
Crystal system	Monoclinic	Orthorhombic	Triclinic	Monoclinic	Monoclinic	Monoclinic
Space group	P2(1)/n	Cmcm	Pī	P2(1)/n	P2(1)/c	P2(1)/n
a, (Å)	13.1581(12)	18.3769(17)	10.8520(11)	0.6830(9)	9.9145(8)	13.2966(14)
b, (Å)	18.089(2)	22.872(2)	12.0573(12)	17.4096(17)	25.3498(18)	18.2077(17)
c, (Å)	18.1897(19)	7.1930(7)	13.4407(13)	26.591(2)	9.1533(7)	17.7183(15)
α, (o)	90	90	86.764(2)	90	90	90
β, (o)	91.2760(10)	90	84.9410(10)	98.1910(10)	116.6190(10)	106.1850(10)
γ, (o)	90	90	79.0670(10)	90	90	90
V, ($Å^3$)	4,328.5(8)	3,023.3(5)	1,718.6(3)	4,895.2(8)	2,056.7(3)	4,119.6(7)
Z	4	4	2	2	4	4
μ(Mo, Kα) (mm^{-1})	1.420	1.358	1.199	1.261	1.005	1.013
Total reflections	21,502	7,526	8,641	8,641	10,336	20,460
Unique	7,634	1,505	5,945	8,607	3,614	7,250
F(000)	2,308	1,600	896	2,540	1,000	1,992
Goodness-of-fit on F^2	1.050	1.079	1.014	1.031	1.029	1.097
R_{int}	0.0376	0.0790	0.0200	0.0573	0.0639	0.0497
$I > 2\sigma(I)$	5,694	1,067	4,078	4,822	1,635	3,218
*R*1	0.0342	0.0480	0.035	0.0555	0.0736	0.0623
$\omega R2$	0.0764	0.1230	0.0688	0.1198	0.2075	0.1710
*R*1 (all data)	0.0550	0.0685	0.0625	0.1142	0.1404	0.1503
$\omega R2$ (all data)	0.0896	0.1467	0.0829	0.1501	0.2347	0.2648
Largest diff. Peak and hole(e/$Å^3$)	0.593, −0.933	1.148, −0.685	0.531, −0.358	1.001, −0.750	0.943, −0.685	1.662, −0.869

Table 2 Selected bond lengths (Å) and angles (°) for compound (1), (2), (3), (4), (5), and (6)

$[Ag_3(bpy)_3](su)]\cdot 10H_2O$ (1)							
Bond lengths (Å)							
Ag(1)–N(2)	2.153(3)	Ag(1)–N(1)	2.155(3)	Ag(2)–N(4)	2.155(3)	Ag(2)–N(3)	2.157(3)
Ag(3)–N(5)	2.184(3)	Ag(3)–N(6)	2.193(3)	Ag(3)–O(3)	2.483(3)		
Bond angles (°)							
N(2)–Ag(1)–N(1)	166.40(12)	N(4)–Ag(2)–N(3)	170.35(12)	N(5)–Ag(3)–N(6)	159.34(12)		
N(5)–Ag(3)–O(3)	99.09(11)	N(6)–Ag(3)–O(3)	96.05(11)				
$[Ag_2(bpy)_2](tp)]\cdot 6H_2O$ (2)							
Bond lengths (Å)							
Ag(1)–N(1)	2.173(6)	Ag(1)–N(2)$^{\#1}$	2.182(6)	N(2)–Ag(1)$^{\#2}$	2.182(6)		
Bond angles (°)							
N(1)–Ag(1)–N(2)$^{\#1}$	176.1(2)						
Symmetry transformations used to generate equivalent atoms: #1 $-x + 3/2, y + 1/2, z$; #2 $-x + 3/2, y - 1/2, z$							
$[Ag_2(dpe)_2(H_2O)_2](dpad)\cdot H_2O$ (3)							
Bond lengths (Å)							
Ag(1)–N(1)	2.143(3)	Ag(1)–N(3)	2.146(3)	Ag(1)–O(1)	2.553(3)		
Ag(2)–N(2)	2.170(3)	Ag(2)–N(4)	2.175(3)	Ag(2)–O(3)	2.467(3)		
Bond angles (°)							
N(1)–Ag(1)–N(3)	161.24(12)	N(1)–Ag(1)–O(1)	98.51(11)	N(3)–Ag(1)–O(1)	100.19(11)		
N(2)–Ag(2)–N(4)	157.45(13)	N(2)–Ag(2)–O(3)	96.35(12)	N(4)–Ag(2)–O(3)	102.18(12)		
N(2)–Ag(2)–O(2)	100.22(11)	N(4)–Ag(2)–O(2)	95.87(11)	O(3)–Ag(2)–O(2)	79.02(11)		
$[Ag_6(dpe)_6(H_2O)_4](tp)_3\cdot 12H_2O$ (4)							
Bond lengths (Å)							
Ag(1)–N(2)	2.126(5)	Ag(1)–N(1)	2.135(5)	Ag(1)–O(7)	2.550(5)	Ag(2)–N(4)	2.141(5)
Ag(2)–N(3)	2.146(5)	Ag(2)–O(8)	2.465(5)	Ag(3)–N(6)	2.128(5)	Ag(3)–N(5)	2.131(5)
Bond angles (°)							
N(2)–Ag(1)–N(1)	165.5(2)	N(2)–Ag(1)–O(7)	97.5(2)	N(1)–Ag(1)–O(7)	96.9(2)		
N(4)–Ag(2)–N(3)	162.3(2)	N(4)–Ag(2)–O(8)	97.35(19)	N(3)–Ag(2)–O(8)	100.3(2)		
N(6)–Ag(3)–N(5)	167.0(2)						
[Ag(bpp)](naa) (5)							
Bond lengths (Å)							
Ag(1)–N(1)	2.173(8)	Ag(1)–N(2)	2.207(8)	Ag(1′)–N(2)	2.116(11)	Ag(1′)–N(1)	2.214(12)
Bond angles (°)							
N(1)–Ag(1)–N(2)	154.7(5)	N(2)–Ag(1′)–N(1)	161.4(6)				
$[Ag_2(bpp)_2](dpad)\cdot 6H_2O$ (6)							
Bond lengths (Å)							
Ag(1)–N(3)	2.131(7)	Ag(1)–N(1)	2.147(7)	Ag(2)–N(2)	2.131(8)	Ag(2)–N(4)	2.142(8)
Ag(2)–O(5)	2.600(11)						
Bond angles (°)							
N(3)–Ag(1)–N(1)	178.3(3)	N(2)–Ag(2)–N(4)	167.5(4)	N(2)–Ag(2)–O(5)	99.0(4)		
N(4)–Ag(2)–O(5)	93.5(4)						

and 2.647(3) Å, respectively; Ag(2)…O(7) = 2.713(3) Å]. The Ag…O distances are thus shorter than their van der Waals contact distance of 3.24 Å [12]. 4,4-Bipyridine (bpy) acts as typical bidentate ligand, linking two Ag atoms via the nitrogens from two pyridyl rings, and the dihedral angles between the pyridyl rings of the same bpy are all ca. 32°. Deprotonated su^{2-} acts as a counterion, balancing the cationic charge of the $[Ag_3(bpy)_3]_n^{3n+}$ chains.

The adjacent cationic chains of $[Ag(1)(bpy)]_n^{n+}$, $[Ag(2)(bpy)]_n^{n+}$, and $[Ag(3)(bpy)]_n^{n+}$ are connected by ligand-unsupported Ag…Ag interactions (Ag(1)…Ag(2) and Ag(2)…Ag(3) = 3.3044(6) Å and 3.3188(6) Å, respectively) into 2D cationic sheets, as shown in Fig. 1b. The deprotonated su^{2-} anions are linked into anionic sheets with the aid of lattice water molecules via intermolecular hydrogen-bonding interactions, as listed in Table 3. The

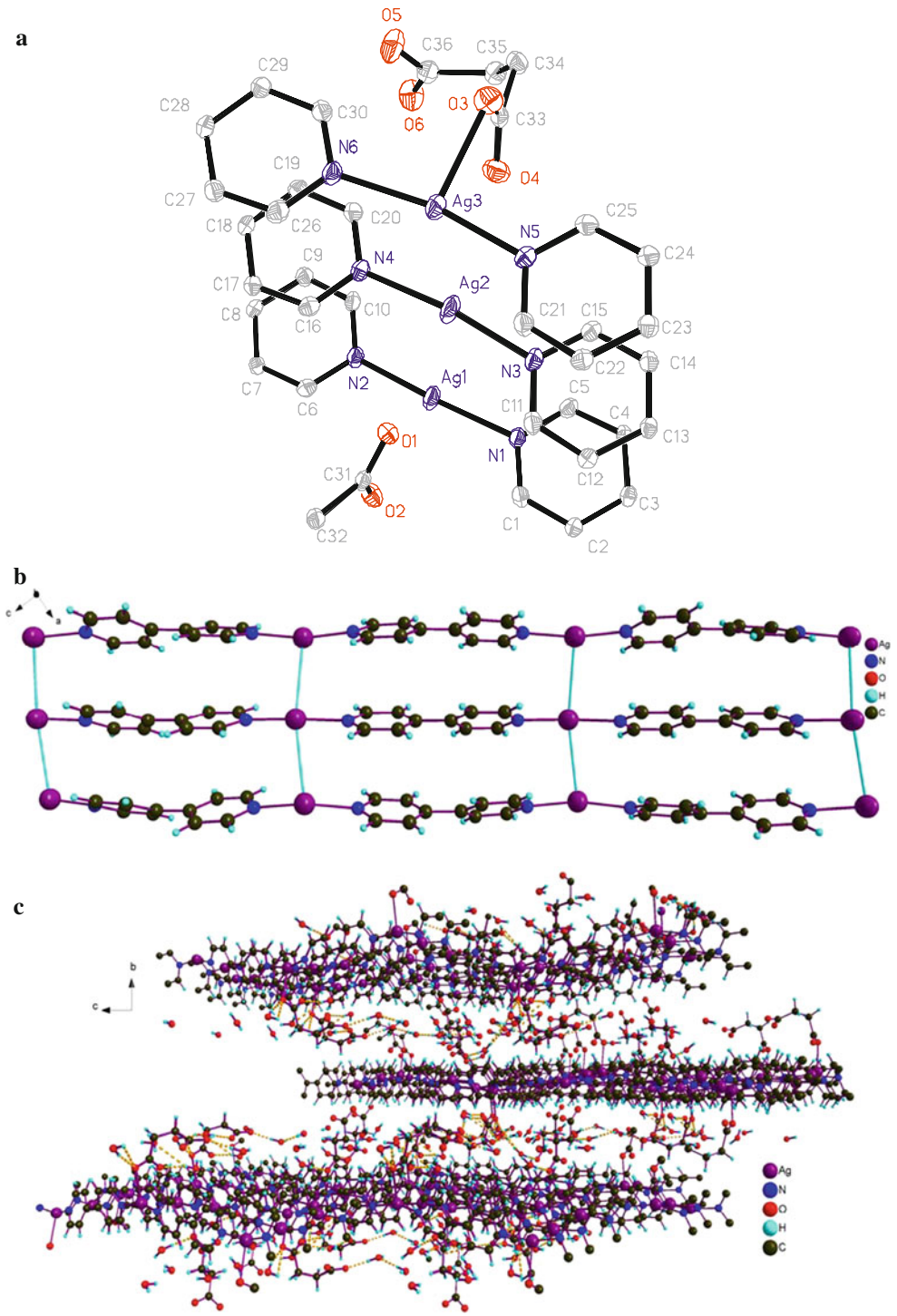

Fig. 1 **a** Ortep view of the structure of $[Ag_3(bpy)_3](su)]\cdot 10H_2O$ (1) with atomic labeling of one asymmetric unit. Lattice water molecules and H atoms are omitted for clarity. **b**. Ag…Ag interactions between neighboring $[Ag(bpy)]^{n+}_{\infty}$ chains in complex (1) (Ag…Ag ranging from 3.529(2) to 3.589(2) Å). **c**. Packing view of the sandwich-like framework built from anionic sheets (B) and cationic sheets (A) along the *a*-axis for 1

neighboring cationic and anionic sheets are further joined into a 3D sandwich-like framework by weak Ag…O interactions, plus π–π stacking interactions with centroid–centriod distances ranging from 3.529(2) to 3.589(2) Å (Table 4) and electrostatic interactions. Viewed from the *c*-axis, it can be seen that the anionic sheet is inserted into the two cationic sheets to form a typical sandwich-like framework.

Table 3 Hydrogen bonds for compound (1), (2), (3), (4), and (6) [Å and °]

D–H	d(D–H)	d(H…A)	<DHA	d(D…A)	A
(1)					
O7–H7C	0.850	2.264	163.84	3.090	O4
O7–H7D	0.850	1.934	162.79	2.757	O6 [$-x + 1, -y + 1, -z + 1$]
O8–H8C	0.850	1.949	169.93	2.790	O5 [$x - 1, y, z$]
O8–H8D	0.850	1.948	170.45	2.790	O5 [$-x + 1, -y + 1, -z + 1$]
O9–H9C	0.850	1.972	168.30	2.809	O8 [$x + 1, y, z$]
O9–H9D	0.850	1.898	167.45	2.734	O3
O10–H10C	0.850	1.855	176.29	2.704	O2 [$x, y - 1, z$]
O10–H10D	0.850	1.992	177.17	2.841	O12 [$-x + 1, -y + 1, -z + 1$
O11–H11C	0.850	1.880	174.07	2.727	O6
O11–H11D	0.850	1.923	173.43	2.769	O14 [$-x + 1, -y + 1, -z + 1$]
O12–H12C	0.850	1.959	170.16	2.800	O1
O12–H12D	0.850	2.074	170.25	2.915	O9 [$-x + 3/2, y + 1/2, -z + 3/2$]
O13–H13C	0.850	2.066	173.36	2.912	O10 [$-x + 1, -y + 1, -z + 1$]
O13–H13D	0.850	1.970	172.64	2.815	O15 [$-x + 1, -y + 1, -z + 1$]
O14–H14C	0.850	2.055	177.19	2.904	O4
O14–H14D	0.850	1.895	176.98	2.743	O16 [$-x + 3/2, y - 1/2, -z + 3/2$]
O15–H15C	0.850	2.085	172.95	2.930	O9 [$-x + 3/2, y - 1/2, -z + 3/2$]
O15–H15D	0.850	1.924	172.50	2.769	O11 [$x - 1/2, -y + 1/2, z + 1/2$]
O16–H16C	0.850	1.990	162.40	2.812	O10 [$-x + 1, -y + 1, -z + 1$]
O16–H16D	0.850	1.952	162.49	2.775	O13 [$-x + 2, -y + 2, -z + 1$]
(2)					
O1–H1C	0.850	1.789	133.48	2.453	O6 [$-x + 3/2, -y + 1/2, -z + 1$]
O1–H1C	0.850	1.952	173.19	2.798	O6 [$-x + 3/2, -y + 1/2, z + 1/2$]
O1–H1D	0.850	2.119	132.53	2.766	O8 [$-x + 3/2, -y + 1/2, -z + 1$]
O1–H1D	0.850	2.122	172.57	2.966	O8 [$x + 1/2, y + 1/2, z$]
O2–H2C	0.850	1.789	120.69	2.340	O3
O2–H2C	0.850	2.066	168.77	2.905	O7
O2–H2D	0.850	2.039	168.98	2.878	O3 [$x, y, -z + 3/2$]
O7–H7C	0.850	2.055	179.01	2.905	O2 [$-x + 1, y, z$]
O7–H7D	0.850	1.636	151.88	2.419	O4
O7–H7D	0.850	1.904	179.51	2.754	O4 [$x, y, -z + 1/2$]
O8–H8C	0.850	1.916	178.23	2.766	O1 [$-x + 3/2, -y + 1/2, -z + 1$]
O8–H8D	0.850	1.728	135.12	2.406	O8 [$x, y, -z + 3/2$]
O8–H8D	0.850	1.886	179.09	2.735	O5 [$x, y, -z + 3/2$]
(3)					
N5–H5	0.860	1.991	134.35	2.664	O6
N5–H5	0.860	2.138	127.24	2.745	O5
O1–H1C	0.850	2.020	165.88	2.852	O2 [$-x + 1, -y + 1, -z + 1$]
O1–H1D	0.850	1.856	164.74	2.686	O6 [$x + 1, y-1, z$]
O2–H2C	0.850	2.058	169.29	2.897	O1 [$x-1, y + 1, z$]
O2–H2D	0.850	1.837	168.66	2.676	O5 [$-x, -y + 2, -z + 1$]
O3–H3C	0.850	1.885	177.54	2.735	O7
O3–H3D	0.850	1.838	177.53	2.687	O4 [$x-1, y, z$]
(4)					
O7–H7B	0.850	2.004	151.55	2.781	O4 [$-x + 1/2, y + 1/2, -z + 3/2$]
O7–H7C	0.850	1.989	150.64	2.761	O5 [$-x + 1, -y + 2, -z + 1$]
O8–H8B	0.850	1.965	148.10	2.724	O1 [$-x, -y + 1, -z + 1$]

Table 3 continued

D–H	d(D–H)	d(H…A)	<DHA	d(D…A)	A
O8–H8C	0.850	2.007	148.02	2.765	O10
O9–H9C	0.850	1.966	178.84	2.816	O5 [$-x+1, -y+1, -z+1$]
O9–H9D	0.850	1.906	178.24	2.756	O12
O10–H10C	0.850	1.878	171.58	2.722	O2 [$x+1, y, z$]
O10–H10D	0.850	1.964	171.88	2.808	O3
O11–H11C	0.850	1.991	173.36	2.836	O4
O11–H11D	0.850	1.943	173.26	2.789	O13 [$x+1/2, -y+3/2, z+1/2$]
O12–H12C	0.850	1.947	165.65	2.778	O11 [$-x+3/2, y-1/2, -z+3/2$]
O12–H12D	0.850	1.871	165.48	2.702	O14 [$-x+3/2, y-1/2, -z+3/2$]
O13–H13C	0.850	1.879	164.42	2.707	O6 [$x-1, y, z$]
O13–H13D	0.850	1.978	164.56	2.807	O6 [$-x+1, -y+2, -z+1$]
O14–H14C	0.850	1.873	172.70	2.718	O3
O14–H14D	0.850	1.904	172.76	2.750	O2 [$x+1, y, z$]
(6)					
N5–H5	0.860	2.037	132.64	2.695	O2
N5–H5	0.860	2.329	112.32	2.773	O4
O5–H5C	0.850	1.845	172.65	2.690	O7 [$x-1/2, -y+3/2, z+1/2$]
O5–H5D	0.850	1.883	173.06	2.729	O10 [$x-1/2, -y+3/2, z+1/2$]
O6–H6C	0.850	1.792	175.86	2.641	O4 [$x+1/2, -y+3/2, z+1/2$]
O6–H6D	0.850	2.068	176.23	2.916	O7 [$x+1/2, -y+3/2, z+1/2$]
O7–H7C	0.850	1.855	168.51	2.694	O2
O7–H7D	0.850	1.991	168.26	2.829	O9 [$-x+3/2, y+1/2, -z+1/2$]
O8–H8C	0.850	1.928	169.40	2.768	O1 [$x, y-1, z$]
O8–H8D	0.850	2.028	169.87	2.869	O1 [$-x+2, -y+1, -z$]
O9–H9C	0.850	1.949	169.58	2.789	O3
O9–H9D	0.850	2.088	169.96	2.928	O8 [$-x+3/2, y+1/2, -z+1/2$]
O10–H10C	0.850	1.937	165.22	2.768	O3
O10–H10D	0.850	2.038	165.68	2.869	O6 [$x-1/2, -y+3/2, z-1/2$]

Crystallographic analysis of complex (2)

$[Ag_2(bpy)_2](tp)\cdot 6H_2O$ (2) is made up of infinite chains of $[Ag_2(bpy)_2]_n^{2n+}$ cations, tp^{2-} anions, and H_2O molecules, as illustrated in Fig. 2a. In the chains of $[Ag_2(bpy)_2]_n^{2n+}$ cations, the Ag^I atoms, in a linear coordination geometry, are coordinated by the two nitrogen atoms from two different bpy ligands [Ag–N bond distances of 2.173(6)–2.182(6) Å; N–Ag–N 176.1(2)°]. The two pyridyl rings of the same bpy ligand are coplanar, different to the bpy ligands in complex (1).

The oxygen atoms of the waters interact with the Ag^I centers through weak Ag…O interactions [Ag(1)…O(1) and Ag(1)…O(2) = 2.633(8) and 2.897(10) Å, respectively]. The deprotonated tp^{2-} anions balance the cationic charges of the $[Ag(bpy)]_n^{n+}$ chains. The COO^- groups are disordered over two positions, such that C(11), C(12), and their corresponding O atoms were split during refinement resulting in a site occupancy factor ratio of 0.50/0.50. The oxygen atoms of the lattice water molecules are also disordered over two positions, such that the site occupancy factor ratios of both O(1)/O(2) and O(7)/O(8) are 0.5/0.5.

Viewed from the *c*-axis, the anionic sheets built up of deprotonated tp^{2-} anions and lattice water molecules via intermolecular hydrogen-bonding interactions (Table 3) are inserted between the two cationic sheets to form a typical sandwich-like framework. No apparent Ag…Ag, Ag…N, or π-π stacking interactions are found in complex 2, which is different from the previously reported similar complexes [2–4, 19].

Crystallographic analysis of complex (3)

As illustrated in Fig. 3a, in the complex $[Ag_2(dpe)_2(H_2O)_2](dpadc)\cdot H_2O$ (3), the Ag(1) and Ag(2) atoms are coordinated in distorted T-shaped coordination geometries by the nitrogen atoms from two different dpe ligands [Ag(1)–N = 2.143(3) and 2.146(3) Å; and Ag(2)–N =

Table 4 Defined ring and relative parameters of the π–π interactions in complexes (1) and (3)

Complex (1)

Cg(1): N(1) → C(1) → C(2) → C(3) → C(4) → C(5) →

Cg(2): N(2) → C(6) → C(7) → C(8) → C(9) → C(10) →

Cg(3): N(5) → C(21) → C(22) → C(23) → C(24) → C(25) →

Cg(4): N(6) → C(26) → C(27) → C(28) → C(29) → C(30) →

Cg(5): N(3) → C(11) → C(12) → C(13) → C(14) → C(15) →

Cg(6): N(4) → C(16) → C(17) → C(18) → C(19) → C(20) →

Cg(I) → Cg(J)	Dist. centroids (Å)	Dihedral angle (°)	Perp. Dist. (IJ) (Å)	Perp. Dist. (JI) (Å)
Cg(1) → Cg(4)	3.550(2)	2.39(17)	3.3785(15)	3.4188(15)
Cg(2) → Cg(5)	3.534(2)	4.91(17)	3.3544(15)	3.4036(15)
Cg(2) → Cg(6)	3.589(2)	3.52(18)	3.3592(15)	3.3170(15)
Cg(3) → Cg(5)	3.537(2)	3.68(18)	3.3310(15)	3.3161(15)
Cg(4) → Cg(6)	3.529(2)	4.49(18)	3.3635(15)	3.3634(15)

Complex (3)

Cg(3): N(3) → C(13) → C(14) → C(15) → C(16) → C(17)–>

Cg(I) → Cg(J)	Dist. centroids (Å)	Dihedral angle (°)	Perp. Dist. (IJ) (Å)	Perp. Dist. (JI) (Å)
Cg(3) → Cg(3)^{i}	3.665(2)	0	3.3652(16)	3.3651(16)

Symmetry codes: (i) $2 - x, -y, 2 - z$

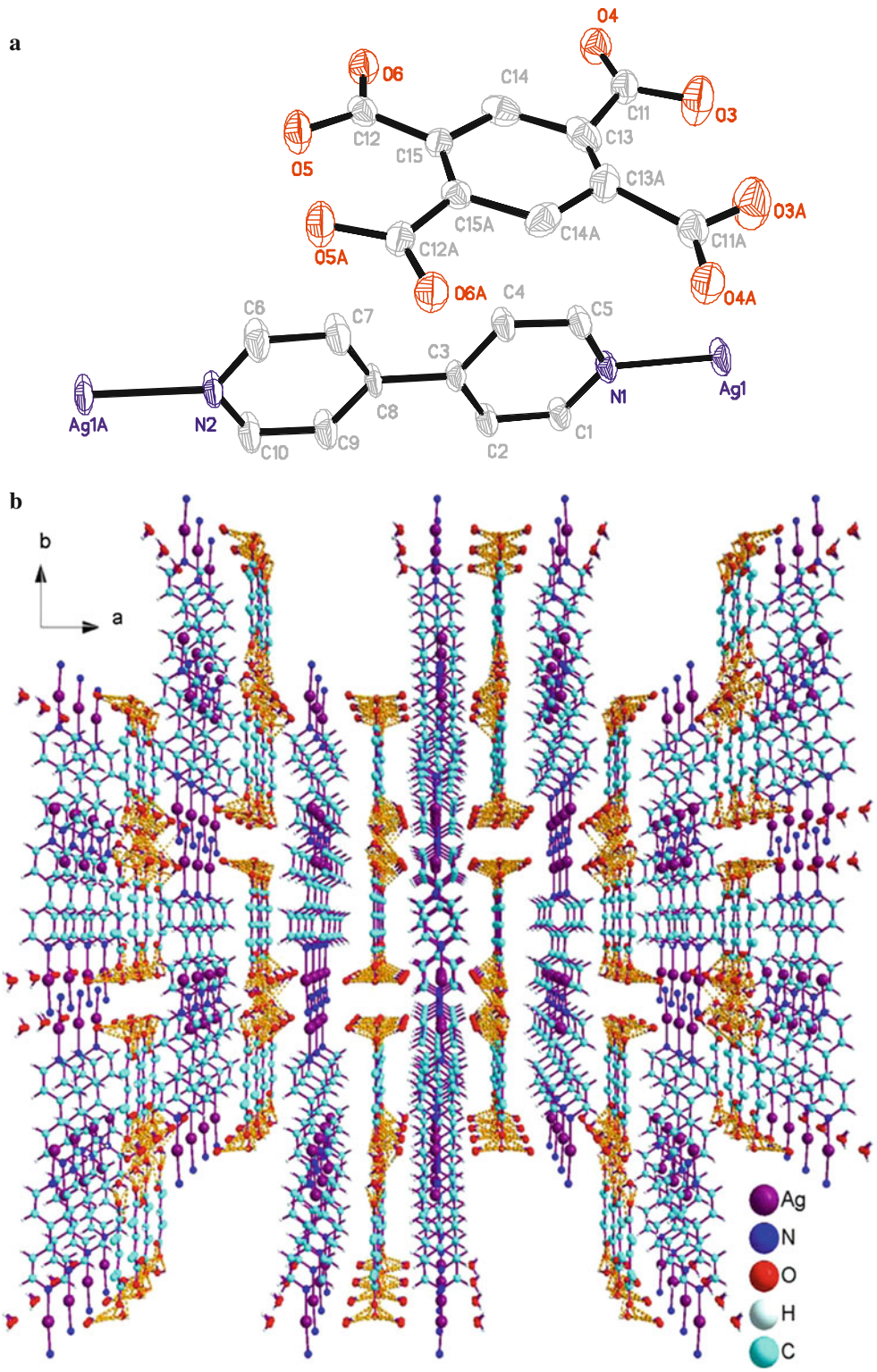

Fig. 2 **a** Asymmetric unit of $[Ag_2(bpy)_2](tp)\cdot 6H_2O$ (2) and coordination environments around the Ag^I atoms. The position occupancy factor ratios of C(11)/C(11A), C(12)/C(12A), O(3)/O(3A), O(4)/O(4A), O(5)/O(5A), and O(6)/O(6A) are 0.50/0.50 (symmetry code: A $-x + 3/2$, $y + 1/2$, z). **b** Packing view of the sandwich-like framework built from anionic and cationic sheets along the *c*-axis for complex (2)

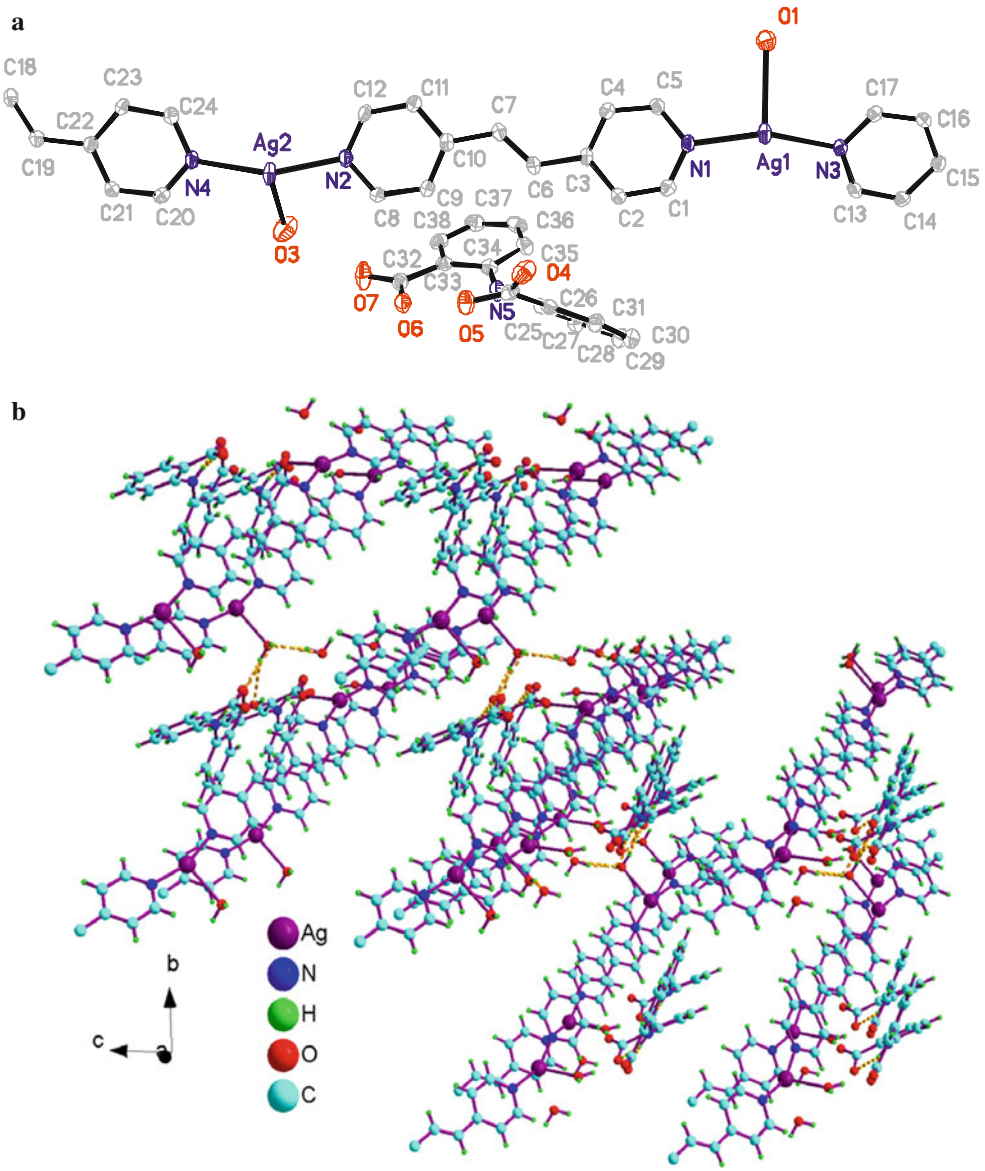

Fig. 3 **a** Asymmetric unit of $[Ag_2(dpe)_2(H_2O)_2](dpadc)\cdot H_2O$ (3) and coordination environments around the Ag^I atoms. **b** Packing view of the sandwich-like framework built from anionic and cationic sheets along the *c*-axis for (3)

2.170(3) Å and 2.175(3) Å; N–Ag(1)–N = 161.24(12)°; N–Ag(2)–N = 157.45(13)°], comparable to the Ag–N distances in previously reported complexes [1–4, 19], and the oxygen atom of an aqua ligands [Ag(1)–O(1) = 2.553(3) and Ag(2)–O(3) = 2.467(3) Å]. The oxygen atoms of the aqua ligands also interact with the Ag(2) centers through weak Ag…O interactions [Ag(2)…O(2) = 2.667(3) Å]. The dihedral angles between the two pyridyl rings of the same dpe, which acts as typical bidentate linker, are 4.475(103)°, and the dihedral angle between the two benzene rings of the $dpadc^{2-}$, which acts as counterion to balance the charge of the cationic $[Ag_2(dpe)_2(H_2O)_2]_n^{2n+}$ chains, is 44.925(112)°.

In the crystal structure of the complex (3), no apparent Ag…Ag or Ag…N interactions are found, which is different from similar complexes [2–4, 19]. The adjacent chains are interconnected by π–π stacking interactions with centroid–centriod distances of 3.665(2) Å (Table 4) and the $dpadc^{2-}$ counterions via electrostatic interactions to build up a 3D sandwich-like network. The lattice water molecules are held within the framework by hydrogen-bonding interactions (Table 3).

Crystallographic analysis of complex (4)

The crystal structure reveals that $[Ag_6(dpe)_6(H_2O)_4](tp)_3\cdot 12H_2O$ (4) is made up of infinite cationic chains of $[Ag_6(dpe)_6(H_2O)_4]_n^{6n+}$, tp^{2-} anions, and H_2O molecules, as illustrated in Fig. 4a. In the cationic chains of $[Ag_6(bpy)_6(H_2O)_4]_n^{6n+}$, the Ag(1) and Ag(2) atoms, in slightly distorted T-shaped geometry, are coordinated by two nitrogen atoms from two different dpe ligands [Ag(1)–N = 2.126(5)

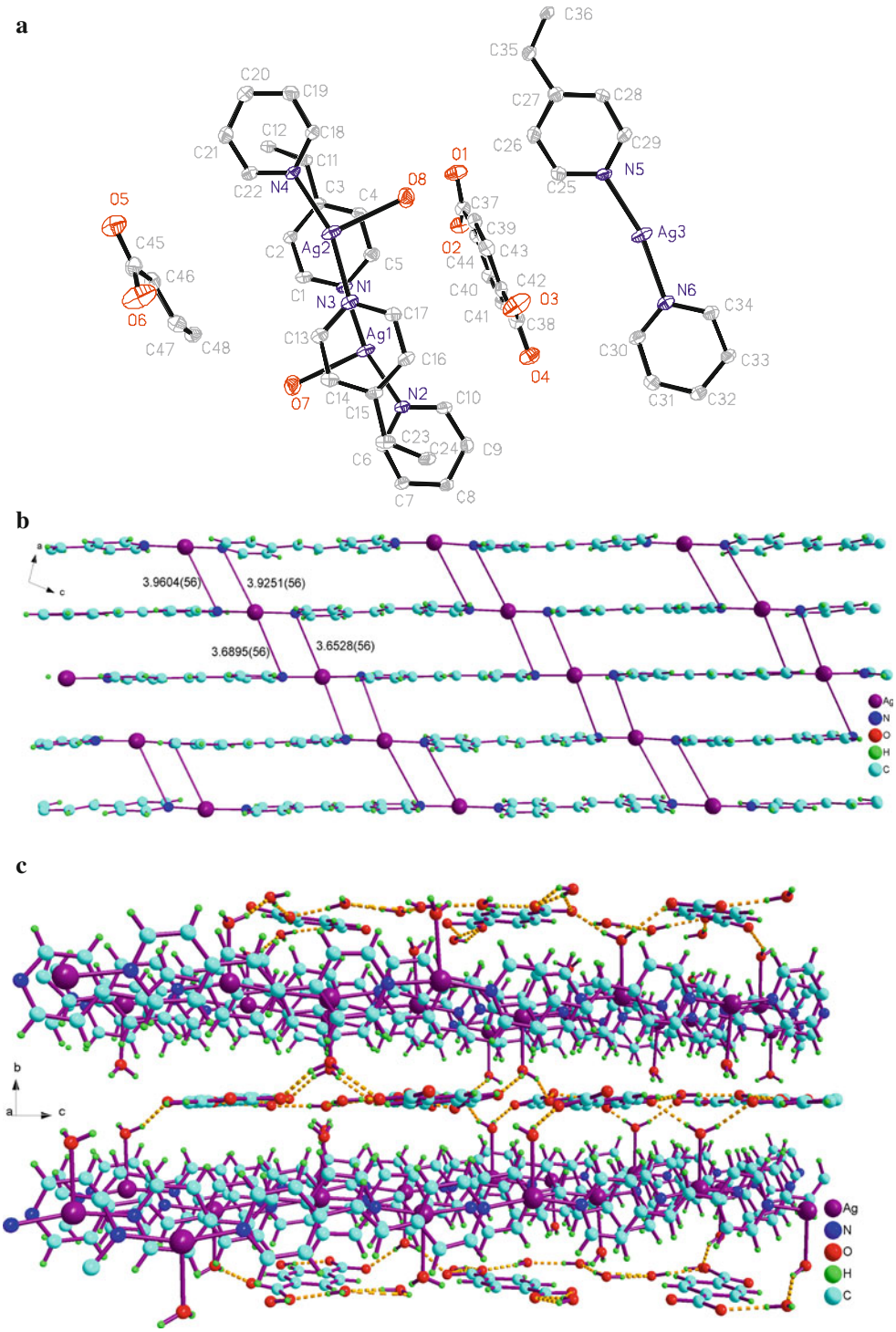

Fig. 4 **a** Asymmetric unit of $[Ag_6(dpe)_6(H_2O)_4](tp)_3 \cdot 12H_2O$ and coordination environments around the Ag^I atoms. **b** The ligand-unsupported Ag…N interactions between the adjacent cationic $[Ag(dpe)]_n^{n+}$ chains. **c** Packing view of the sandwich-like framework built from anionic and cationic sheets along the *a*-axis for (4)

and 2.135(5) Å; Ag(2)–N = 2.141(5) and 2.146(5) Å; N–Ag(1)–N = 165.5(2)° and N–Ag(2)–N = 162.3(2)] and by an oxygen atom from an aqua ligand [Ag(1)–O = 2.550(5) Å and Ag(2)–O = 2.465(5) Å], as illustrated in Fig. 1a and Table 2. Meanwhile, the Ag(3) atoms, in linear coordination geometry, are coordinated by two nitrogen atoms from two different dpe ligands [Ag–N = 2.128(5) and 2.131(5) Å; N–Ag1–N = 165.5(2)° and N–Ag2–N = 167.0(2)°]. The oxygen atom of the aqua ligand interacts weakly with Ag(3) ions [Ag(2)…O(2) = 2.609(6) Å]. In all the dpe ligands, the two pyridyl rings are nearly coplanar, the corresponding dihedral angles being 0.581(270)°, 6.734(280),° and 1.779(229)°.

The adjacent cationic $[Ag(dpe)]_n^{n+}$ chains are connected by Ag…N interactions (Ag…N contacts ranging from 3.6528(56) to 3.9604(56) Å) into 2D cationic sheets, as shown in Fig. 4b. The deprotonated tp^{2-} anions are joined into anionic sheets with the aid of lattice water molecules via intermolecular hydrogen-bonding interactions, as depicted in Table 3. The neighboring cationic and anionic sheets are further joined into a 3D sandwich-like framework by hydrogen-bonding and electrostatic interactions.

Crystallographic analysis of complex (5)

The crystal structure reveals that [Ag(bpp)](naa) (5) is made up of infinite sinusoidal cationic chains of $[Ag(bpp)]_n^{n+}$ and naa^- anions, as illustrated in Fig. 5a. In the cationic chains of $[Ag(bpp)]_n^{n+}$, the Ag atoms are disordered over two positions; hence, the Ag(1) and Ag(1)′ atoms were split during refinement resulting in a site occupancy factor ratio of 0.74(2)/0.26(2). Both Ag(1) and Ag(1)′, in linear coordination geometry, are coordinated by the nitrogen atoms from two different bent bpp ligands [Ag(1)–N = 2.173(8) and 2.207(8) Å; Ag(1)′–N = 2.214(12) and 2.116(11) Å; N–Ag(1)–N = 154.7(5)° and N–Ag(1)′–N = 161.4(6)°], as illustrated in Fig. 5a and Table 2. The oxygen atoms of the naa^- anions interact with the Ag^I centers through weak Ag…O interactions [Ag…O = 2.681(17) and 2.771(15) Å], which are shorter than their van der Waals contacts distance of 3.24 Å. The bent bpp ligand acts as a flexible linker to join two Ag^I atoms, such that the dihedral angle between the two pyridyl rings is 70.649(224)°, while the naa^- anions provide charge compensation.

The adjacent cationic $[Ag(bpp)]_n^{n+}$ chains are connected by ligand-unsupported Ag…Ag interactions (Ag(1)–Ag(1)$(-x+1, -y+1, -z+1)$ = 3.040(9) Å and Ag(1)′–Ag(1) $(-x+1, -y+1, -z+1)$ = 2.854(19) Å) into 2D cationic sheets. The deprotonated naa^- anions contact the cationic $[Ag(bpp)]_n^{n+}$ chains via weak Ag…O interactions to build a 3D sandwich-like crystal structure, as depicted in Table 3.

Crystallographic analysis of complex (6)

In $[Ag_2(bpp)_2](dpadc)\cdot 6H_2O$ (6), the Ag(1) atoms have a linear coordination geometry involving the nitrogen atoms from two different bent bpp ligands [Ag–N bond distance being 2.131(7)–2.147(7) Å; N–Ag–N 178.3(3)°], forming simple sinusoidal cationic chains. The oxygen atoms of aqua ligands interact with the Ag^I centers through weak Ag…O interactions [Ag(1)…O(1) = 2.781(8) Å], while the Ag(2) atoms, in slightly distorted T-shape, are ligated by the nitrogen atoms from two different bpp ligands [Ag–N = 1.131(8) and 2.142(8) Å, N–Ag–N = 167.5(5)°] and the oxygen from an aqua ligand [Ag–O = 2.600(11) Å, N–Ag–O = 99.0(4) and 93.5(4)°]. The dihedral angle between the two pyridyl rings of bpp linkers is 73.41(29),° comparable to that in complex (5). The deprotonated $dpadc^{2-}$ anions balance the charge of the $[Ag_2(bpp)_2]_n^{2n+}$ cationic chains, as illustrated in Fig. 6. And the dihedral angle between the two benzene rings of $dpadc^{2-}$ is 45.152(34)°, similar to the angles in complex (3).

In the complex (6), no apparent Ag…Ag, Ag…N, or π–π stacking interactions are found, which is different from similar complexes [2–4, 19]. The adjacent chains are interconnected by the $dpadc^{2-}$ counterions via electrostatic interactions to build up a 3D sandwich-like network. The lattice water molecules are held within the framework and stabilized by hydrogen-bonding interactions (Table 3).

Some complexes of silver(I) with bpy-like ligands but different counterions have been reported previously [1–4, 19]. The coordination modes of the ligands and the supramolecular interactions of the anions both help to determine the crystal structures of such complexes. Generally, the counterions can be present in coordinated, uncoordinated, or mixed modes. Coordinated anions normally increase the dimensionality of the crystal structures, while uncoordinated anions may help to extend the crystal structures via hydrogen bonding, π–π stacking, and/or ligand-unsupported Ag…Ag and Ag…N interactions. For example, in $Ag(bpe)_2(bpdc)_2$ (bpe = 1,2-bis(4-pyridyl) ethane, H_2bpdc = 2,2′-bipyridine-3,3′-dicarboxylic acid), the $bpdc^{2-}$ acts as a coordinated counterion, linking the Ag(I) atoms into a 3D framework along with the bpe ligands [19]. In construct, in $[Ag_2(bpe)_2](bdc)\cdot 8H_2O$ (H_2bdc = 1,3-benzenedicarboxylic acid), bdc^{2-} only plays the role of an uncoordinated counterion to balance the charge of the 1D cationic $[Ag_2(bpe)_2]^{2+}$ chains. Again, the 3D sandwich-like structure of $[Ag_2(bpe)_2](bdc)\cdot 8H_2O$ is constructed with the aid of Ag…Ag, Ag…N, and hydrogen-bonding interactions [19].

Conclusions

The six silver(I) complexes reported here all contain novel sandwich-like frameworks, showing that the different anions play an important role in determining the crystal structures. In these complexes, the rigid bpy and flexible dpe/bpp act as bidentate ligands to join the Ag(I) centers into 1D cationic chains, balanced by the different anions, like su^{2-}, tp^{2-}, $dpadc^{2-}$, and naa^-. The coordination numbers of silver are two and three, resulting in linear (complex (1–2), (4–6)) or T-shape (complexes (1), (3), (4), and (6)) geometries. All the organic carboxylate anions only act as counterions to balance the charge of the cationic $[Ag(L)]_n^{n+}$ chains. In complexes (1), (4), and (5), the

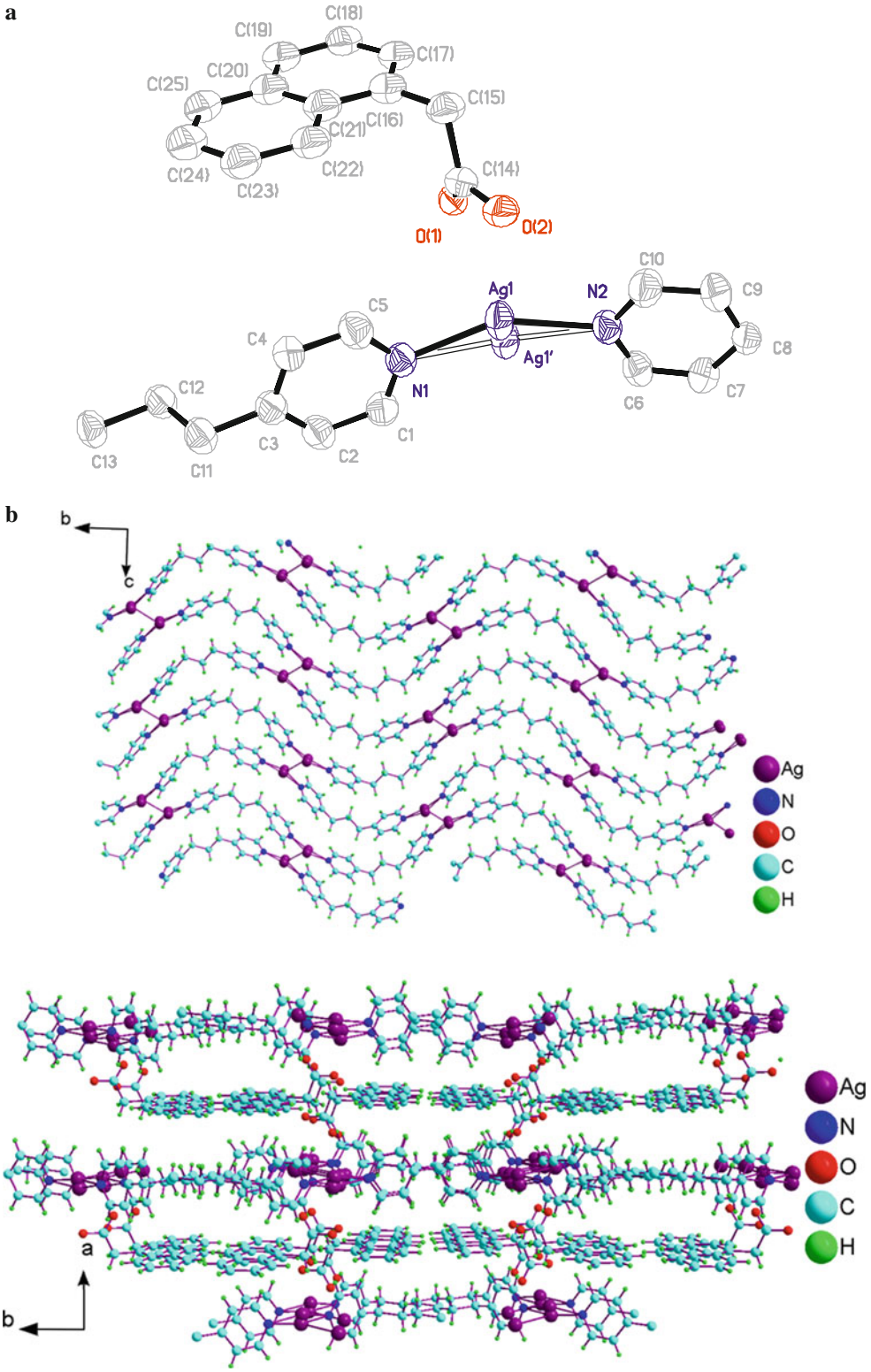

Fig. 5 **a** Asymmetric unit of [Ag(bpp)](naa) (5) and coordination environments around the Ag^{I} atoms. **b** The ligand-unsupported Ag…Ag interactions between adjacent cationic $[Ag(bpp)]_n^{n+}$ chains. **c** Packing view of the sandwich-like framework built from anionic and cationic sheets along the *c*-axis for (5)

ligand-unsupported Ag…Ag and Ag…N interactions facilitate the formation of 3D sandwich-like structures, generally supported by rich hydrogen-bonding interactions. In complexes (1) and (3), besides the abundant hydrogen bonds, π–π stacking interactions also contribute to the formation of a 3D sandwich-like framework.

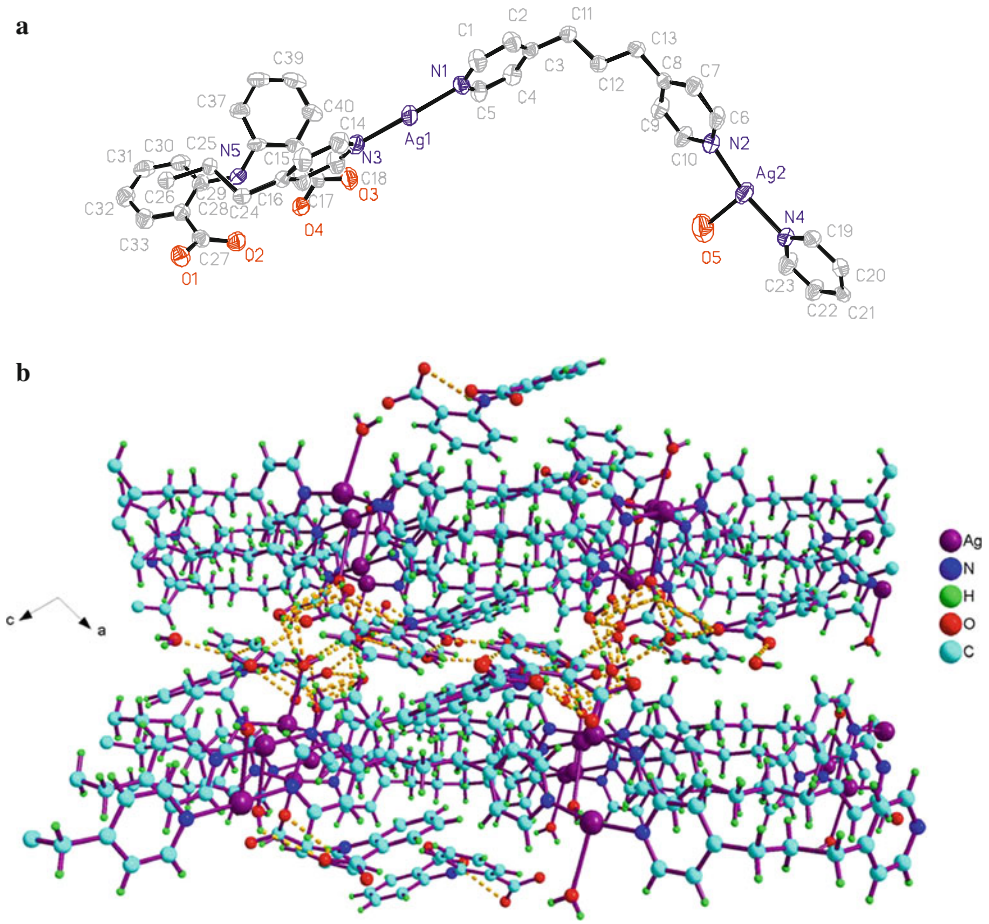

Fig. 6 **a** Asymmetric unit of $[Ag_2(bpp)_2](dpadc)\cdot 6H_2O$ (6) and coordination environments around the Ag^I atoms. **b** Packing view of the sandwich-like framework built from anionic and cationic sheets along the *c*-axis for (6)

Supplementary material

CCDC 860827-860832 contain the supplementary crystallographic data for this paper. These data can be obtained free of charge from The Cambridge Crystallographic Data Centre via http://www.ccdc.cam.ac.uk/data_request/cif.

Acknowledgments The study was financially supported by Funding Project for Academic Human Resources Development in Institutions of Higher Learning Under the Jurisdiction of Beijing Municipality (Grant No. PHR201008372 and PHR201106124) and Open Research Fund Program of Key Laboratory of Urban Stormwater System and Water Environment (Ministry of Education), Beijing University of Civil Engineering and Architecture (Grant No. YH201101003).

References

1. Chen CL, Kang BS, Su CY (2006) Aust J Chem 59:3–18
2. Wang CC, Wang P, Guo GS (2010) Transition Met Chem 35:721–729
3. Wang CC, Song YX, Wang YL, Wang P (2011) Chinese J Inorg Chem 27(2):361–366
4. Wang CC, Wang P (2011) Chinese J Struct Chem 30(6):811–818
5. Zhang JP, Kitafawa S (2008) J Am Chem Soc 130:907–917
6. Kascatan-Nebioglu A, Panzner MJ, Tessier CA, Cannon CL, Youngs WJ (2007) Coord Chem Rev 251:884–895
7. Zhang YN, Wang H, Liu JQ, Wang YY, Fu AY, Shi QZ (2009) Inorg Chem Commun 12:611–614
8. Yin PX, Zhang J, Li ZJ, Qin YY, Cheng JK, Zhang L, Lin QP, Yao YG (2009) Cryst Growth Des 9:4884–4896
9. Ni J, Wei KJ, Liu YZ, Huang XC, Li D (2010) Cryst Growth Des 10:3964–3976
10. Chen W, Du M, Bu XH, Zhang RH, Mak TCW (2003) Cryst Eng Comm 5:96–100
11. Tong ML, Wu YM, Ru J, Chen XM, Chang HC, Kitagawa S (2002) Inorg Chem 41:4846–4848
12. Yeh CW, Chen TR, Chen JD, Wang JC (2009) Cryst Growth Des 9:2595–2602
13. Park KM, Seo J, Moon SH, Lee SS (2010) Cryst Growth Des 10:4148–4154
14. Zheng XF, Zhu LG (2009) Cryst Growth Des 9:4407–4414
15. Degtyarenko AS, Solntsev PV, Krautscheid H, Rusanov EB, Chernega AN, Domasvitch KV (2008) New J Chem 32: 1910–1918
16. Wu H, Dong XW, Ma JF, Liu HY, Yang J, Bai HY (2009) Dalton Trans 2009:3162–3174
17. Haftbaradaran F, Draper ND, Leznoff DB, Williams VE (2003) Dalton Trans 2003:2105–2106

18. Munakata M, Wu LP, Kuroda-Sowa T, Mackawa M, Suenaga Y, Ohta T, Konaka H (2003) Inorg Chem 42:2553–2558
19. Wang CC, Wang P, Feng LL (2012) Transit Met Chem 37(2): 225–234
20. Sheldrick GM (1997) SADABS, program for empirical absorption correction of area detector data. University of Göttingen, Germany
21. Sheldrick GM (1997) SHELXS 97, program for crystal structure solution. University of Göttingen, Germany
22. Sheldrick GM (1997) SHELXL 97, program for crystal structure refinement. University of Göttingen, Germany
23. Allen FH (2002) Acta Crystallogr Sect B: Struct Sci 58:380–388
24. Allen FH, Davies JE, Galloy JJ, Johnson O, Kennard OF, Macrae C, Mitchell EM, Mitchell GF, Smith JM, Watson JDG (1991) Chem Inf Comput Sci 31:187–204
25. Safaa EE, Ahmed SBE (2011) Transit Met Chem 36(1):13–19